ISSN 1029-9599, Physical Mesomechanics, 2016, Vol. 19, No. 1, pp. 107–114. © Pleiades Publishing, Ltd., 2016.
Original Russian Text © M.P. Kashchenko, V.G. Chashchina, 2014, published in Fizicheskaya Mezomekhanika, 2014, Vol. 17, No. 5, pp. 63–70.

Orientations of Type II Twin Boundaries in B2→B19′ Martensitic Transformation in Dynamic Theory

M. P. Kashchenko[1,2]* and V. G. Chashchina[1,2]

[1] *Ural Federal University, Ekaterinburg, 620002 Russia*
[2] *Ural State Forest Engineering University, Ekaterinburg, 620100 Russia*
** e-mail: mpk46@mail.ru*

Received January 31, 2014

Abstract—The paper analyzes the possibility of describing the orientations of type II twin boundaries in B2→B19' martensitic transformation in the framework of dynamic theory based on the concepts of heterogeneous nucleation and wave growth of martensite crystals. It is shown that the twin boundary orientations can be defined by strain fields in crystal contact regions characteristic of self-accommodated groups with common $\langle 001\rangle_{B2}$ poles.

DOI: 10.1134/S1029959916010112

Keywords: dynamic theory, martensitic transformation, titanium nickelide, type II twins, morphological characteristics

1. INTRODUCTION

Progress in the description of γ→α martensitic transformation features in iron alloys within a paradigm developed elsewhere [1] raises the question as to whether the developed methodology can be applied to transformations in titanium nickelide, for which the first-order transition features are less pronounced. Recall that the key role in dynamic theory [1] belongs to the idea of the initial excited (oscillatory) state that appears in the elastic fields of dislocation nucleation centers and governs the controlling wave process. The wave process disturbs lattice stability, and transition of the lattice to a new equilibrium state is accompanied by the formation of unambiguously related morphological features (orientation of habit planes, orientation relations, macroshear) that bear some information about the cooperative transformation process. Habit planes (with normal $\mathbf{N}_w$) have the simplest description: it is sufficient to know the wave normals $\mathbf{n}_1$ and $\mathbf{n}_2$ of controlling wave beams along the orthogonal directions of eigenvectors $\boldsymbol{\xi}_i$ ($i = 1, 2$) of the strain tensor of the elastic field of a defect and the wave velocity ratio κ:

$$\mathbf{N}_w \| \mathbf{n}_2 - \mathbf{n}_1\kappa,\ |\mathbf{n}_{1,2}| = 1,\ \kappa = v_2/v_1. \qquad (1)$$

The calculation of orientation relations and macroshear requires transition to final strains [1]. The transition was first carried out within dynamic theory for bcc to hcp transformation for titanium [2, 3]. An important requirement in this case is that the ratio of tensile strains ε_1 ($\varepsilon_1 > 0$) and compressive strains ($\varepsilon_2 < 0$) specified by the threshold wave process must remain constant. For purely longitudinal waves propagating along the symmetry axes (or in an isotropic medium) we have:

$$k = \varepsilon_1/|\varepsilon_2| \approx \kappa^2. \qquad (2)$$

Taking into account quasi-longitudinal waves, relation (2) can be generalized; in so doing, k is not reduced to a simple equation with κ^2 but is naturally related with it.

According to the classification (see, e.g., [4]) for titanium nickelide alloys, there are three variants of transformations: B2→B19, B2→R, B2→B19′. The latter variant can occur at several combinations of instability channels. Corresponding elementary cells of phases are displayed in Fig. 1 taken from [4].

The description of habit planes using Eq. (1) is also simple for titanium nickelide alloys. For example, the habits of type $\{223\}_{B2}$–$\{334\}_{B2}$ observed in B2→B19 transformation in Ti–Ni–Cu alloys [4] are unambiguously associated with dislocation nucleation centers, with the main dislocation lines segments $\boldsymbol{\Lambda}$ being collinear with $\langle 1\,\bar{1}0\rangle_{B2}$ directions [5]. Less symmetric orientations of $\{0.39\ 0.48\ 0.78\}_{B2}$ habits were observed for the B19′ phase. They can be associated with the nucleation processes in elastic fields at $\boldsymbol{\Lambda}$ collinear with $\langle\bar{2}01\rangle_{B2}$ directions. This was reasonably explained by Letuchev

et al. for aged alloys in which Ti_3Ni_4 phase particles precipitate [6]. Such habits can also be associated with both $\mathbf{\Lambda}_1 \| \langle 1\,\bar{1}\,0\rangle_{B2}$ and $\mathbf{\Lambda}_2 \| \langle 1\,1\,\bar{1}\rangle_{B2}$ [7–10] if taking into account that the orientation $\mathbf{\Lambda}$ is modified in transition to intermediate states (particularly in B2→B19 transition).

A more complex task is to interpret the observed various orientations of transformation twin boundaries [4] in the B19′ phase, especially type II twin boundaries (using an irrational description of boundary orientations), which is carried out in this paper.

2. DESCRIPTION OF {10*h*} TWIN BOUNDARY ORIENTATIONS

Recall that the $\{110\}_\gamma$ twin boundary orientations in γ→α transformation in iron alloys are described similarly to habits using Eq. (1) [11, 12]. In the equation, the $\langle 100\rangle_\gamma$ and $\langle 010\rangle_\gamma$ wave normals are associated with relatively short-wave *s*-displacements acting in consistency with relatively long-wave *l*-displacements that are responsible for the formation of habits, and $\kappa_s = 1$. Such twin boundaries refer to type I that corresponds to a rational description of boundary orientations. According to Miyazaki et al., the transformation twins usually observed in contacting crystals (e.g., in pyramidal B19' phase crystals) refer to type II [13]. There are variants with boundary orientations [13]:

$$\{\bar{1}\ 0\ 2.4\}_{B2} \| \{\overline{0.72}\ 1\ 1\}_{B19'}. \quad (3)$$

The boundary orientations for crystals and twins are schematically illustrated in Fig. 2 taken from [13]. Miyazaki et al. define intervals of orientations for $\{10h\}_{B2}$ twin boundaries at $|h| > 1$, with the central parts of the intervals approximately corresponding to $h = \pm 2$ [13].

The zero Miller index in the notation of twin boundary orientation in the B2 phase axes allows the orientations to be described by Eq. (1) using a pair of unit orthogonal wave normals (lying, e.g., in the $(100)_{B2}$ plane) as:

$$\mathbf{n}_1'(\theta) = [0\ \ \cos\theta\ \ \sin\theta]_{B2},$$
$$\mathbf{n}_2'(\theta) = [0\ -\sin\theta\ \cos\theta]_{B2}. \quad (4)$$

Normals (4) are primed to discriminate them from the normals $\mathbf{n}_1$ and $\mathbf{n}_2$ of wave beams that specify habit

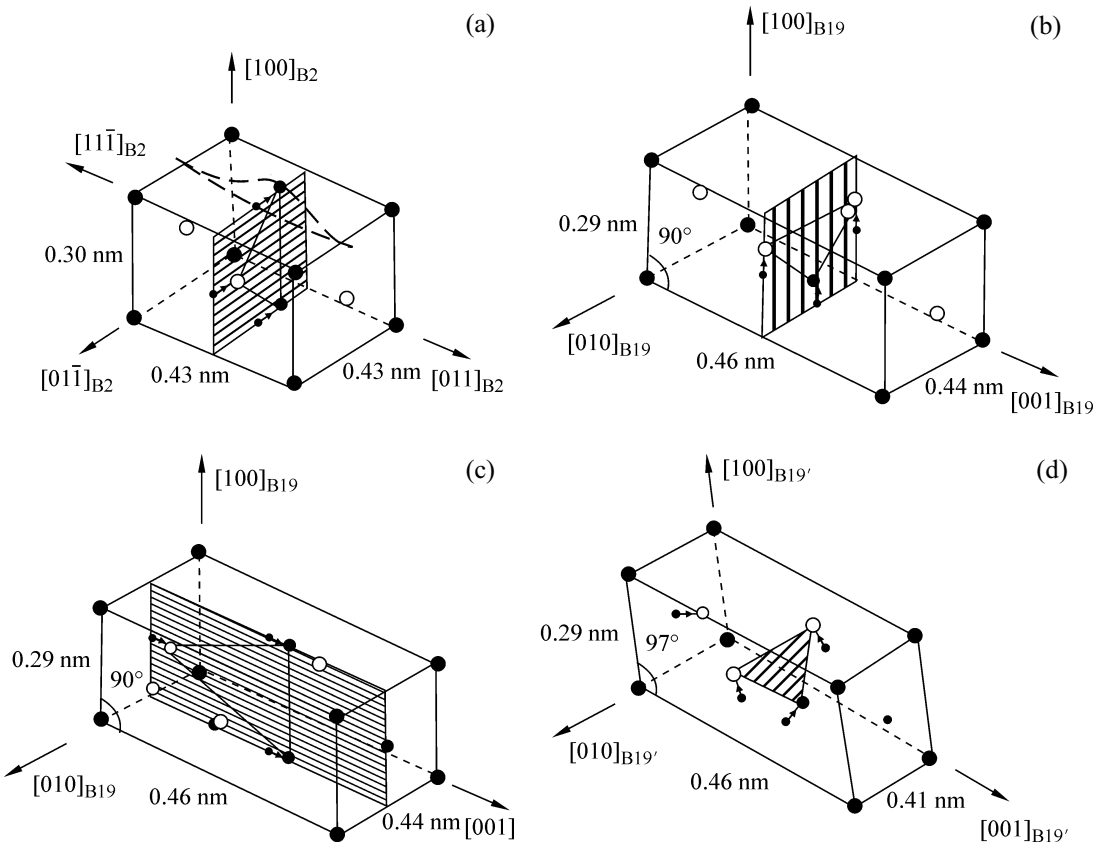

Fig. 1. Elementary cells of B2 (a), B19 (b, c) and B19′ phases (d) in titanium nickelide alloys, their dimension to orientation ratios, and schematic transformations determined by shuffle ($\{011\}\langle 100\rangle$ and $\{01\,\bar{1}\}\langle 100\rangle$) atomic displacements ($\{011\}_{B2}$ shear planes are hatched). The figure corresponds to Fig. 3.12 from [7].

planes. Notice that the velocities of waves of the same polarization in mutually orthogonal directions in the $(100)_{B2}$ plane are equal to each other. Consequently, strains must also be equal according to Eq. (2). Substituting Eq. (4) into Eq. (1), at $\kappa = 1$, we find:

$$\mathbf{N}'_{w} \parallel \mathbf{n}'_2(\theta) \pm \mathbf{n}'_1(\theta)$$
$$\parallel [0\ (\cos\theta \mp \sin\theta)\ (\sin\theta \pm \cos\theta)]_{B2}. \quad (5)$$

Particularly, at $\mathbf{n}'_1(0) = [010]_{B2}$ and $\mathbf{n}'_2(0) = [001]_{B2}$ the twin boundaries coincide with $(01\bar{1})_{B2}$ or $(011)_{B2}$, while at $\mathbf{n}'_1(\pi/4) \parallel [011]_{B2}$ and $\mathbf{n}'_2(\pi/4) \parallel [0\bar{1}1]_{B2}$ they coincide with $(010)_{B2}$ or $(001)_{B2}$. The normal to boundary (3) is collinear with $\mathbf{n}'_2(\theta) - \mathbf{n}'_1(\theta)$ at $\theta = \arctan(1/3) \approx 18.435°$, where

$$\begin{aligned} \mathbf{n}'_1(\theta) &= [\cos\theta\ \ 0\ \ \sin\theta]_{B2} \\ &\approx [0.948683\ \ 0\ \ 0.316228]_{B2}, \\ \mathbf{n}'_2(\theta) &= [\sin\theta\ \ 0\ \ -\cos\theta]_{B2} \\ &\approx [0.316228\ \ 0\ \ -0.948683]_{B2}. \end{aligned} \quad (6)$$

However, the boundary of type (3) can also be represented by the difference $\mathbf{n}'_2 - \mathbf{n}'_1$ in which wave normals have no zero projections.

Hence the defined role of $\mathbf{n}'_{1,2}$ directions of type (6) requires separate physical justification.

3. PHYSICAL REASONS FOR DEFINING WAVE NORMAL DIRECTIONS IN SHORT-WAVE TWINNING SHEAR

The general idea of dynamic theory implies that wave normals must be specified by eigenvectors of the strain tensor of the elastic field that breaks the symmetry of the initial phase. It is therefore makes sense to verify the hypothesis about the role of elastic deformation in the contact area between crystals in the formation of type II twins. First, it is reasonable to describe the possible dynamic pattern of individual crystal formation through the B2→B19→B19′ channel, assuming that transition to the intermediate B19 structure occurs according to the wave mode that satisfies Eqs. (1) and (2). We assume that the transition occurs as in the case of bcc to hcp transformation [3, 4] with the most rapid deformation of the $(01\bar{1})_{B2}$ planes during wave propagation that induces compressive and tensile deformation close to the $[100]_{B2}$ and $[011]_{B2}$ symmetry axes, respectively.

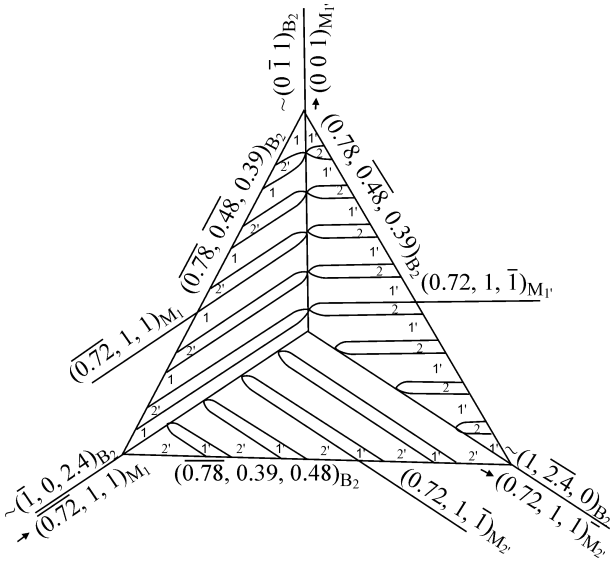

Fig. 2. Orientation of type II twin boundaries in junction of three crystals [13].

Estimation is performed using lattice parameters [14] for Ti–40Ni–10Cu system:

$$\begin{aligned} a_{B2} &= 0.3030\ \text{nm},\ a_{B19} = 0.2881\ \text{nm}, \\ b_{B19} &= 0.4279\ \text{nm},\ c_{B19} = 0.4514\ \text{nm}. \end{aligned} \quad (7)$$

The given values of parameters (7) differ greatly from the data represented in Fig. 1 for qualitative illustration. Strains on edges of the B2 phase cell are given by the relations

$$\begin{aligned} \varepsilon_{[100]} &= (a_{B19} - a_{B2})/a_{B2}, \\ \varepsilon_{[01\bar{1}]} &= (b_{B19} - \sqrt{2}a_{B2})/(\sqrt{2}a_{B2}), \\ \varepsilon_{[011]} &= (c_{B19} - \sqrt{2}a_{B2})/(\sqrt{2}a_{B2}). \end{aligned} \quad (8)$$

Equations (8) and (7) yield the following values for the basis of the B2 phase:

$$\begin{aligned} \varepsilon_{[100]} &\approx -0.04917,\ \varepsilon_{[01\bar{1}]} \approx -0.00142, \\ \varepsilon_{[011]} &\approx 0.05343. \end{aligned} \quad (9)$$

It is evident from Eq. (9) that the most rapid compressive and tensile deformation in the orthogonal $[100]_{B2}$ and $[011]_{B2}$ direction occurs in the $(01\bar{1})_{B2}$ plane (the strain $\varepsilon_{[01\bar{1}]} \approx -0.00142$ is low). Assuming that $\varepsilon_1 = \varepsilon_{[011]} \approx 0.05343$ and $\varepsilon_2 = \varepsilon_{[100]} \approx -0.04917$, we have:

$$\varepsilon_1 / |\varepsilon_2| \approx 1.0865. \quad (10)$$

The calculation of parameter κ using data on elastic moduli of Ti_{50}–Ni_{38}–Cu_{10}–Fe_2 single crystals yields $\kappa^2 \approx 0.8872$ for the case of wave normals directed along the symmetry axes, which is smaller than value (10), and hence Eq. (2) is not satisfied. Nevertheless, at deviation from the symmetry axes with regard to quasi-longitudinal *l*-waves the values of parameters *k* and κ can be naturally correlated. A detailed consideration of the issue is beyond the scope of this work.

The most significant difference of the B19′ phase from the B19 phase, which is obvious from comparison of Figs. 1b and 1d, is that one of the cell edges loses orthogonality with respect to the two other edges. This

factor should be taken into account in further analysis. In addition to elementary cell strains (9), we should take into account shear strain in the $(100)_{B2}$ plane along the $[011]_{B2}$ direction which leads to monoclinic distortion of the orthorhombic lattice. Recall that simple shear strain in the coordinate-free form reads [11, 12]:

$$\hat{T} = \hat{l} + S\,\boldsymbol{\tau}\cdot\mathbf{n},\quad S = \tan\psi = 2\tan\omega,\ \tau = n = 1, \qquad (11.1)$$

$$\hat{T} = \hat{\lambda}\hat{\omega}. \qquad (11.2)$$

In Eq. (11.1) $\hat{l}$ is the unit tensor, $\boldsymbol{\tau}\cdot\mathbf{n}$ is the dyadic notation of shear strain in the plane with normal $\mathbf{n}$ in the $\boldsymbol{\tau}$ direction, with the shear value S, and ω is the angle of rotation about the $[\boldsymbol{\tau}, \mathbf{n}]$ axis ([,] is the symbol of vector product). In Eq. (11.2) $\hat{\lambda}$ and $\hat{\omega}$ are the strain and rotational components of tensor $\hat{T}$ at its polar decomposition.

For definiteness, we give the matrix notation of the resulting distortion tensor $\hat{\chi}$ in the basis $[100]_{B2}$, $[011]_{B2}$, $[01\bar{1}]_{B2}$ at strain (9) (omitting low strain $\varepsilon_{[01\bar{1}]}$) and shear along the $(100)_{B2}$ plane in the $[011]_{B2}$ direction:

$$\chi_{ij} = \begin{bmatrix} \varepsilon_{[100]} & 0 & S \\ 0 & 0 & 0 \\ 0 & 0 & \varepsilon_{[011]} \end{bmatrix}. \qquad (12)$$

The basis with the given orientation of axes along the edges of the B2 phase cell will be denoted by the symbol B19. In order to obtain the strain tensor $\hat{\varepsilon}$ at low values of the matrix elements, it is enough to isolate the symmetric part in Eq. (12):

$$\varepsilon_{ij} = 1/2(\chi_{ij} + \chi_{ji})$$

$$= \begin{bmatrix} \varepsilon_{[100]} & 0 & S/2 \\ 0 & 0 & 0 \\ S/2 & 0 & \varepsilon_{[011]} \end{bmatrix} = \begin{bmatrix} \varepsilon_{[100]} & 0 & \tan\omega \\ 0 & 0 & 0 \\ \tan\omega & 0 & \varepsilon_{[011]} \end{bmatrix}. \qquad (13)$$

As was shown elsewhere [2, 3, 8, 9], the development of transformation is related to shear that leads to material rotation by angle φ depending on κ. A variant of notation of the analytical dependence $\varphi(\kappa)$ reads:

$$\varphi(\kappa) = \arccos\frac{\Gamma + \kappa^2}{\sqrt{(\Gamma^2 + \kappa^2)(\kappa^2 + 1)}}, \qquad (14)$$

$$\Gamma = \frac{1 + \varepsilon_1}{1 - |\varepsilon_2|}.$$

In the considered case, the angle $\varphi(\kappa)$ describes the rotation of the frame $\langle 100\rangle_{B2}, \langle 01\bar{1}\rangle_{B2}$ about the $\langle 011\rangle_{B2}$ axis (with retained orthogonality of initial edges $\langle 100\rangle_{B2}$ and $\langle 01\bar{1}\rangle_{B2}$ during rotation). In a more general case, compared to Eq. (2), the notation of Eq. (14) can be retained with the replacement of $\kappa \to k$. Then, substituting $k^2 \approx 1.0865$, $\varepsilon_1 \approx 0.05343$, $|\varepsilon_2| \approx 0.04917$ into Eq. (14) we find $\Gamma \approx 1.107906$ and $\varphi(k) \approx 2.934°$.

It is naturally conceivable that the developing shear $\tan\psi$ that breaks the orthogonality of the initial edges $\langle 100\rangle_{B2}$ and $\langle 01\bar{1}\rangle_{B2}$, according to Eq. (11), must be close to $2\tan\varphi(k)$.

Now let us discuss the possibility of appearance of twins with non-typical boundary orientations in twin contacts. Deformation in the contact area is described by the sum of strains associated with individual contact regions. Then, instead of Eq. (13), we come to:

$$\varepsilon_{ij} \approx \begin{bmatrix} 2\varepsilon_{[100]} & \tan\omega & \tan\omega \\ \tan\omega & \varepsilon_{[011]} & 0 \\ \tan\omega & 0 & \varepsilon_{[011]} \end{bmatrix}$$

$$\approx \begin{bmatrix} -0.09834 & 0.05125 & 0.05125 \\ 0.05125 & 0.05343 & 0 \\ 0.05125 & 0 & 0.05343 \end{bmatrix}. \qquad (15)$$

The eigenvalues of tensor (15) and corresponding eigenvectors are:

$$\varepsilon_1 = 0.082484,\ \varepsilon_2 = -0.127394,\ \varepsilon_3 = 0.05343,$$
$$\xi_1 \| [0.372063 \quad 0.656342 \quad 0.656342]_{B19},$$
$$\xi_2 \| [0.928208 \quad -0.263088 \quad -0.263088]_{B19}, \qquad (16)$$
$$\xi_3 \| [0 \quad -0.707107 \quad 0.707107]_{B19}.$$

Passing on to the basis $\langle 100\rangle_{B2}$ (through rotation about $[100]_{B2}$ by angle $\pi/4$), we have:

$$\xi_1 \| [0.372063 \quad 0.928208 \quad 0]_{B2},$$
$$\xi_2 \| [0.928208 \quad -0.372063 \quad 0]_{B2}, \qquad (17)$$
$$\xi_3 \| [0 \quad 0 \quad 1]_{B2}.$$

Then,

$$\mathbf{n}_2' - \mathbf{n}_1' = \xi_2 - \xi_1 \| [0.556145 \quad -1.300271 \quad 0]_{B2}$$
$$\| [1 \quad -2.338007 \quad 0]_{B2},$$
$$\mathbf{n}_2' + \mathbf{n}_1' = \xi_2 + \xi_1 \| [1.300271 \quad 0.556145 \quad 0]_{B2} \qquad (18)$$
$$\| [2.338007 \quad 1 \quad 0]_{B2}.$$

Result (18) corresponds to a slight deviation (by angle $\approx 1°$) from the orientation $[1\ \overline{2.4}\ 0]_{B2}$ proposed by Miyazaki et al. [13] and to deviation by angle $\approx 4°$ from the orientation $[1\ \bar{2}\ 0]_{B2}$. The existence of the orientation interval is evidently due to the variation of angle ω associated, according to Eq. (11), with the rotational component of shear that characterizes monoclinic distortion. For example, at unchanged diagonal elements of matrix (15) in the limiting case $\omega \to 0$ $|h| \to 1$, i.e., boundary orientations

tend to $\{101\}_{B2}$. In another limiting case of $\omega \to \varphi(k)$, the inequality $|h| > 2$ holds true. Clearly, the variation of ω at unchanged diagonal elements is formal because the value of ω depends on strains. The loss of stability to monoclinic shear in the region that transforms by the B2→B19 scenario most probably occurs when the value of φ exceeds a certain value φ_{th} that, conceivably, divides the linear and nonlinear elasticity domains. Hence strain growth at the initial stage of unstable lattice relaxation is not necessarily accompanied by monoclinic shear, but at $\varphi > \varphi_{th}$ shear takes place and increases up to $2\tan\omega \approx 2\tan\varphi(\kappa)$.

The last conclusion generally agrees with experimental data. Really, the angle value in monoclinic distortion is defined to be ≈96.8°, i.e., the shear value in angular measurement corresponds to ≈6.8°. With the above estimate for the angle $\varphi(\kappa) \approx 2.934°$, the difference of $2\varphi(k)$ from 6.8° is less than by 1°. However, we must be aware of experimental errors in measuring lattice parameters and elastic moduli (by which we estimated strains, κ and $\varphi(k)$) as well as of the fact that our consideration refers to temperature M_s. Recall that the value of monoclinic distortions increases away from M_s (during cooling).

It should be noted that the dependence $\varphi(k)$ in the domain of low strains is linear with respect to strains (at fixed k). Really,

$$\varphi(k) \approx \frac{180\, k\, (\varepsilon_1 + |\varepsilon_2|)}{\pi\,(k^2+1)}. \qquad (19)$$

The quantity $\varphi(k)$ in Eq. (19) is measured in degrees. With regard to $k^2 = \varepsilon_1/|\varepsilon_2|$ we have $\varphi(k) \approx k\,|\varepsilon_2|$ from Eq. (19), where $\varphi(k)$ is measured in radians. Then, the non-diagonal elements in matrix (17) take the form:

$$\tan\omega = \tan\varphi(k) \approx k\,|\varepsilon_2|. \qquad (20)$$

Now substituting Eq. (20) in matrix (15) shows that in order to find the sought eigenvectors we should diagonalize the matrix that contains only parameter k. Assuming that $\varepsilon_{[01\bar{1}]} = 0$, $2\varepsilon_{[100]} = -2|\varepsilon_2|$, and $\varepsilon_{[011]} = \varepsilon_1$, we turn to the simplest notation of the matrix that has the same eigenvector orientations as matrix (15) in accordance with the sequence of changes in matrix notation:

$$\varepsilon_{ij} \to \begin{bmatrix} -2|\varepsilon_2| & |\varepsilon_2|\,k & |\varepsilon_2|\,k \\ |\varepsilon_2|\,k & \varepsilon_1 & 0 \\ |\varepsilon_2|\,k & 0 & \varepsilon_1 \end{bmatrix}$$

$$\to \begin{bmatrix} -2 & k & k \\ k & k^2 & 0 \\ k & 0 & k^2 \end{bmatrix} \to \begin{bmatrix} -2/k & 1 & 1 \\ 1 & k & 0 \\ 1 & 0 & k \end{bmatrix}. \qquad (21)$$

Using matrix (21), we can easily calculate index h that specifies boundary orientations for type II twins $\{10h\}_{B2}$ depending on k. Recall that when calculating boundary orientations for type II twins $\{10h\}_{B2}$ both wave vectors of s-waves lie in one of the $\{100\}_{B2}$ symmetry planes, s-wave velocities are equal, and $\kappa_s = 1$. Hence orientations of normals to the $\{10h\}_{B2}$ boundaries according to Eq. (5) are collinear with the sum or difference of eigenvectors of matrix (21). Table 1 illustrates the dependence $h(k)$ and gives eigenvector orientations in the basis of the initial B2 phase. For completeness it also represents the case of $k < 1$ ($\kappa_j < 1$ can be observed in materials with the elastic anisotropy factor $A < 1$).

The bolded values in the table correspond to the value $k \approx 1.043$ that has been discussed above. It is interesting that at simultaneous observation of deformation by monoclinic shear the h values exceed 2, at least at realistic k values for the considered materials which are close to the given above. Probably, at fixed k the range of h values with the central point $h = 2$ is governed by a retarded increase of monoclinic shear with respect to strains. This can be illustrated by introducing parameter y ($0 \le y \le 1$) to the last matrix (21) instead of unit nondiagonal elements. The above-said is an illustration for the data in Table 2 obtained at the fixed value $k \approx 1.043$.

The performed calculations demonstrate that orientations of type II twin boundaries can be described by pairs of s-waves propagating from contact regions in twin crystals.

Table 1. Dependence of index h that specifies twin boundary orientation on parameter k

k	$\mathbf{n}_1'$			$\mathbf{n}_2'$			$\mathbf{n}_3'$	h
0.8	0.34693	0.93789	0	0.93789	–0.34693	0	001	2.174
0.9	0.35978	0	0.93304	0.93304	0	0.35978	001	2.255
1	0.369	0.92941	0	0.929	–0.369	0	001	2.318
1.043	**0.372**	**0.928**	**0**	**0.928**	**0.372**	**0**	**001**	**2.338**
1.1	0.37546	0.92684	0	0.92684	–0.37546	0	001	2.362
1.2	0.37958	0.92516	0	0.92516	0	–0.37958	010	2.392

Table 2. Dependence of index h on variable y that characterizes possible delay of monoclinic shear with respect to strains at $k \approx 1.043$

y	$\mathbf{n}_1'$			$\mathbf{n}_2'$			$\mathbf{n}_3'$	h
1.1	0.394	0.919	0	0.919	–0.394	0	001	2.506
1.0	0.372	0.928	0	0.928	–0.372	0	001	2.338
0.8	0.321	0.947	0	0.947	–0.321	0	001	2.023
0.5	0.221	0.975	0	0.975	–0.221	0	010	1.586
0.0	0	1	0	1	0	0	001	1

4. DISCUSSION OF RESULTS

It is clear that the $(1\ \overline{\sqrt{2}}\ \overline{\sqrt{2}})_{\mathrm{B19}}$ plane with irrational indices corresponds to the exact $(1\ \overline{2}\ 0)_{\mathrm{B2}}$ twin boundary orientation in the basis B19. Twins with such planes are formally referred to type II twins as distinct from type I twins with rational twinning shear planes with rational indices. Evidently, it is more pertinent to associate this term with the specific initial stage of twin formation. In the considered variant (let it be the first variant), the main component of twin structure originates from the contact area of two B19 crystals. At the same time, type I twins are localized in the central part of the front of the controlling wave process. Since matrix (21) contains only one parameter k, s-waves can already be excited in the threshold mode for l-waves and at the formation of type II twins.

There is a second variant when the formation of type II twins starts from contact regions of a crystal of phase B19 (or B19′) with the initial B2 phase. In this case, however, s-wave vector directions are most probably defined by elastic fields of discontinuities (because perfect coherent conjugation of different lattices is impossible). The discontinuities correspond to microterraces between lattices of contacting phases along the densest crystallographic segments of planes. Clearly, the conjugation in the form of "terraces" does not correspond to the threshold mode but to the achievement of final strains [1, 11]. Since this kind of conjugation corresponds (macroscopically) to a single habit plane, the distribution of formed discontinuities must be quasi-regular. Then, if the quasi-regular discontinuities are modeled by a system of dislocation loops, we can find nucleation centers of twin lamellae, and the regular arrays of twins in the scheme in Fig. 2 must be correlated with the characteristic size of the loop. This variant of twin formation will be considered in a separate paper.

The second variant is also interesting when considering plastic deformation of a material transformed by the B2→B19 (B19′) scenario because the current system of discontinuities can become nucleation centers of both single dislocations and their cryston superpositions [14–16]. Moreover, the multitude of twinning processes in shape memory alloys, including mechanical twinning under external stresses, makes for the accumulation of additional elastic energy through a hierarchy of structural levels [17]. For highly reversible processes, strain can be recovered to a degree that exceeds the inherent resource of martensitic reaction, as it was observed elsewhere [18, 19]. Recall that account for structural hierarchy is crucial for the description of deformation processes [20].

Finally, within the conventional crystal geometry approach applied to the B2→B19′ transformation the calculated habits $\{0.89\ 0.22\ 0.40\}_{\mathrm{B2}}$ in [13, 21] in twinning shear of the second type, like

$$\{0.85294\ 0.27789\ 0.43012\}_{\mathrm{B2}}$$

in twinning shear of the first type in [21], greatly deviate from the observed $\{0.78\ 0.39\ 0.48\}_{\mathrm{B2}}$. There is no such problem in dynamic description. Really, the nature of habit plane, particularly in reconstructive martensitic transformations, is purely dynamic. The volume ratio of the main and twin components (at least for type I twins) is given by correlating strains carried by short-wave and relatively long-wave displacements inherent in the controlling wave process [11, 12]; it is not a parameter that fulfils the requirement of macroscopic invariance of habit plane [22]. It is clear that the observed change in the volume ratio of type I twin components within one crystal (with fixed habit) discloses an inconsistency between the crystal geometry approach and physical reality. Hence the formation mechanism of type II transformation twins requires independent analysis in the framework of dynamic theory.

5. CONCLUSION

The performed analysis showed that the dynamic theory of martensitic transformations, which was initially developed to disclose the physical nature of cooperative

γ–α transformation in iron alloys, can also be applied to describe B2→B19 and B2→B19′ martensitic transformations in titanium nickelide alloys. The formation of habit planes, like in the case of iron alloys, is associated with pairs of relatively long quasi-longitudinal waves (wave lengths ~0.1–1.0 μm) inherent in the controlling wave process. These waves specify the mesoscale of the order of thickness of formed martensite crystals. Additional features of B2→B19′ transformation associated with the formation of type II twins are also adequately described in the framework of wave description. However, unlike in the formation mechanism of type I twins, pairs of relatively short waves (wave lengths ~10 nm) responsible for the formation of fine type II twin structure start to propagate from the vicinity of contact between formed crystals. (Earlier, we discussed the possibility to describe type II twins in the framework of dynamic theory [23].)

ACKNOWLEDGMENTS

The work was carried out at the financial support of RFBR (Project No. 14-08-00734).

REFERENCES

1. Kashchenko, M.P. and Chashchina, V.G., Dynamic Model of Supersonic Martensitic Crystal Growth, *Physics-Uspekhi*, 2011, vol. 54, no. 4, pp. 331–349.
2. Kashchenko, M.P. and Chashchina, V.G., Crystal Dynamics of the bcc–hcp Martensitic Transformation: I. Controlling Wave Process, *Phys. Met. Metallog.*, 2008, vol. 105, no. 6, pp. 537–543.
3. Kashchenko, M.P. and Chashchina, V.G., Crystal Dynamics of the bcc–hcp Martensitic Transformation: II. Morphology, *Phys. Met. Metallog.*, 2008, vol. 106, no. 1, pp. 14–23.
4. Pushin, V.G., Prokoshkin, S.D., Valiev, R.Z., Brailovski, V. et al., *Titanium Nickelide Shape Memory Alloys. Part I. Structure, Phase Transformations and Properties*, Yekaterinburg: UrB RAS Publ., 2006.
5. Kashchenko, M.P., Aleksina, I.V., Letuchev, V.V., and Nefedov, A.V., Dislocation Centers of Nucleation in B2→B19 Martensitic Transformation of Titanium Nickelide, *Fiz. Met. Metalloved.*, 1995, vol. 80, no. 6, pp. 10–15.
6. Letuchev, V.V., Vereshchagin, V.P., Alexina, I.V., and Kashchenko, M.P., Conception of New Phase Dislocation-Based Nucleation at Recontructive Martensitic Transformations, *J. Phys. IV. Colloq. C8*, 1995, vol. 5, pp. 151–156.
7. Kashchenko, M.P. and Chashchina, V.G., Dynamic Model of Crystal Formation at B2→B19→B19′ Martensitic Transformations, *Proc. of the XVIII St. Petersburg Reading on Strength Problems*, St. Petersburg, October 21–24, 2008, Part II, pp. 153–155.
8. Kashchenko, M.P. and Chashchina, V.G., Dynamic Model of the Formation of an Intermediate Mesoscopic State during B2→B19 Martensitic Transformation, *Russ. Phys. J.*, 2013, vol. 56, no. 5, pp. 557–561.
9. Kashchenko, M.P. and Chashchina, V.G., Dynamic Model of the B2→B19′ Martensitic Transformations Taking into Account an Intermediate Mesoscopic State, *Russ. Phys. J.*, 2013, vol. 56, no. 6, pp. 647–651.
10. Kashchenko, M.P. and Chashchina, V.G., Dynamic Model of B2→B19→ B19′ Martensitic Transformation in Titanium Nickelide, *Met. Sci. Heat Treat.*, 2014, vol. 55, no. 11–12, pp. 643–646.
11. Kashchenko, M.P. and Chashchina, V.G., *Dynamic Model for Formation of Twinned Martensitic Crystals upon γ–α Transformation in Iron-Based Alloys*, Yekaterinburg: USFEU, 2009.
12. Kashchenko, M. and Chashchina, V., *Dynamic Theory of γ→α-Martensitic Transformation in Iron-Based Alloys. Solving the Problem of the Formation of Twinned Martensite Crystals*, Saarbrucken: LAMBERT Academic Publishing, 2012.
13. Miyazaki, S., Otsuka, K., and Wayman, C.M., The Shape Memory Mechanism Associated with the Martensitic Transformation in Ti–Ni Alloys. I. Self-Accomodation, *Acta Metall.*, 1989, vol. 37, no. 7, pp. 1873–1884.
14. Kashchenko, M.P., Semenovykh, A.G., and Chashchina, V.G., Cryston Model of Formation of Strain-Induced Alpha-Martensite in Fe-Based Alloys, *Fiz. Mezomekh.*, 2003, vol. 6, no. 3, pp. 37–56.
15. Kashchenko, M.P., Semenovykh, A.G., and Chashchina, V.G., Cryston Model of Shear Band Formation in Cubic Crystals with Crystallographic Orientation of Random-Type Boundaries, *Fiz. Mezomekh.*, 2003, vol. 6, no. 1, pp. 95–122.
16. Kashchenko, M.P., Letuchev, V.V., Yablonskaya, T.N., and Teplyakova, L.A., A Model of the Formation of Macroshear Bands and Strain-Induced Martensite with (*hhl*) Boundaries, *Phys. Met. Metallog.*, 1996, vol. 2, no. 4, pp. 329–336.
17. Kashchenko, M.P., Konovalov, S.V., and Chashchina V.G., Symmetric Model Evaluation of the Resource of Elastic Energy Stored by an Ensemble of Self-Similar Martensite Crystals, *Met. Sci. Heat Treat.*, 2012, vol. 54, no. 7–8, pp. 355–359.
18. Ryklina, E.P., Prokoshkin, S.D., Chernavina, A.A., and Perevoshchikova, N.N., Investigation on the Influence of Thermomechanical Conditions of Induction and Structure on the Shape Memory Effects in Ti–Ni Alloy, *Inorg. Mat. App. Res.*, 2010, vol. 1, no. 3, pp. 188–194.
19. Ryklina, E.P., Prokoshkin, S.D., and Chernavina, A.A., Peculiarities of Implementation of Abnormally High Shape Memory Effects in Thermomechanically Treated Ti–Ni Alloys, *Inorg. Mat. App. Res.*, 2013, vol. 4, no. 4, pp. 348–355.

20. Panin, V.E. and Egorushkin, V.E., Curvature Solitons as Generalized Structural Wave Carriers of Plastic Deformation and Fracture, *Phys. Mesomech.*, 2013, vol. 16, no. 4, pp. 267–286.
21. Knowles, K.M. and Smith, D.A., The Crystallography of the Martensitic Transformation in Equiatomic Nickel-Titanium, *Acta Metall.*, 1981, vol. 29, pp. 101–110.
22. Kashchenko, M.P. and Chashchina V.G., Key Role of Transformation Twins in Comparison of Results of Crystal Geometric and Dynamic Analysis for Thin-Plate Martensite, *Phys. Met. Metallog.*, 2013, vol. 114, no. 10, pp. 821–825.
23. Kashchenko, M.P. and Chashchina, V.G., Dynamic Theory of the Formation of Second-Order Twins at the B2→B19 Martensitic Transformation in NiTi-Based Alloys, *Proc. of the Int. Symp. "Physics of Crystals 2013" for the 100^h Anniversary of Prof. M.P. Shaskolskaya*, Moscow: NRTU "MISIS", 2013, p. 97.